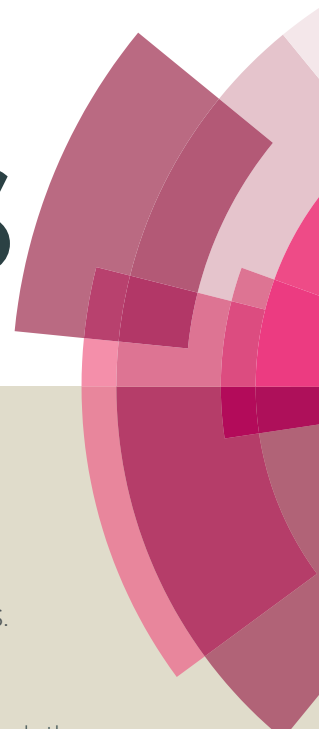


RSC Advances



This article can be cited before page numbers have been issued, to do this please use: D. Sang, H. Li, S. Cheng, Q. Wang, J. Liu, Q. Wang, S. Wang, C. Han, K. Chen and Y. Pan, *RSC Adv.*, 2015, DOI: 10.1039/C5RA06054K.



This is an *Accepted Manuscript*, which has been through the Royal Society of Chemistry peer review process and has been accepted for publication.

Accepted Manuscripts are published online shortly after acceptance, before technical editing, formatting and proof reading. Using this free service, authors can make their results available to the community, in citable form, before we publish the edited article. This *Accepted Manuscript* will be replaced by the edited, formatted and paginated article as soon as this is available.

You can find more information about *Accepted Manuscripts* in the [Information for Authors](#).

Please note that technical editing may introduce minor changes to the text and/or graphics, which may alter content. The journal's standard [Terms & Conditions](#) and the [Ethical guidelines](#) still apply. In no event shall the Royal Society of Chemistry be held responsible for any errors or omissions in this *Accepted Manuscript* or any consequences arising from the use of any information it contains.

HPSTAR
097-2015

View Article Online

DOI: 10.1039/C5RA06054K

Ultraviolet photoelectrical properties of *n*-ZnO nanorods/*p*-diamond heterojunction

Dandan Sang^{a,b}, Hongdong Li^{*b}, Shaoheng Cheng^b, Qiliang Wang^b, Junsong Liu^b, Qinglin Wang^{*c}, Shuang Wang^{b,d}, Chong Han^a, Kai Chen^a, and Yuewu Pan^a

^aMathematics and Physical Sciences Technology, Xuzhou Institute of Technology, Xuzhou 221008, China

^bState Key Laboratory of Superhard Materials, Jilin University, Changchun 130012, China. E-mail: hdli@jlu.edu.cn

^cCenter for High Pressure Science and Technology Advanced Research, Changchun 130012, China. E-mail: wangql@hpstar.ac.cn

^dAviation Institute, Shandong Jiaotong University, Jinan 250357, China

Abstract

The Ultraviolet (UV) photoresponse properties of *n*-ZnO nanorods/*p*-diamond heterojunction were investigated by studying the dark and photo *I*-*V* characteristics. It shows typical rectifying behavior with a rectification ratio of 3.2 and 8.8 for the dark current and the photocurrent, respectively. The turn on voltage under UV illumination is lower by three times than that under the dark current and the ideality factor of the device is decreased. The forward current under UV illumination is more than 4 times higher than the dark one at 10 V whereas the leakage current shows a little increase at -10 V. The electrical transport behaviors are investigated both under the dark current and the photocurrent. The photogenerated charges and their transfer processes were analyzed by surface photovoltage (SPV) measurements.

RSC Advances Accepted Manuscript

1. Introduction

Zinc oxide (ZnO) is a promising candidate for the optoelectronic applications such as ultraviolet (UV) photodetectors,^{1,2} photovoltaic devices,³ and light-emitting diodes⁴ due to its direct wide band gap (3.37 eV) and high exciton binding energy (60 meV). The as-grown ZnO is intrinsically an *n*-type semiconductor and the obtainment of *p*-type conductivity in ZnO remains a major challenge. Due to the deep acceptor level, low solubility of the dopants and the self-compensation process,⁵ the fabrication of a *p-n* homojunction is still a problem. Therefore, ZnO based *p-n* heterojunction is essential for an optoelectronic device. Thus far, heterostructure UV photodetectors have been demonstrated by growing *n*-type ZnO on top of a variety of *p*-type layers such as Si,^{6,7} GaN,^{8,9} SiC,¹⁰ NiO^{11,12}, Cu₂O¹³ and organic material¹⁴. It is known that diamond is an ideal semiconductor for high-power and high temperature optoelectronic devices due to its large band gap (5.47 eV) and highest thermal conductivity. Up to the present, the constructions¹⁵ and the photocatalytic activities¹⁶ based on *n*-ZnO/*p*-diamond heterojunctions have been studied, but the reports on the UV photoelectrical properties of the composited ZnO and diamond *p-n* junction are very limited, which are mainly focused on the ZnO films.^{17,18} Since one-dimensional ZnO nanorods (NRs) can enhance the performance of UV photodiodes due to the large surface area to volume ratio,¹⁹ the *n*-ZnO nanorods deposited on *p*-type diamond film as heterojunction for photodetectors were scarcely tackled and this motivated the present work: by studying the dark and UV photo current-voltage (*I-V*) characteristics, we investigated the UV photoresponse properties of *n*-ZnO nanorods/*p*-diamond heterojunction. The photogenerated charges and the transfer process were analyzed by surface-photovoltage (SPV)

measurements.

2. Experiments

Prior to the growth of ZnO NRs, the *p*-type B-doped diamond (BDD) film with a thickness of $\sim 4 \mu\text{m}$ was fabricated on silicon ($8 \text{ cm} \times 8 \text{ cm}$) by microwave CVD methods. $\text{B}(\text{OCH}_3)_3$ was introduced as the doping source in the reaction atmosphere of methane and hydrogen (CH_4/H_2). The fabrication of ZnO NRs on BDD substrate was carried out by thermal vapor transport method in a quartz tube inserted into a horizontal tube furnace. Mixed raw powders of ZnO and aluminum (Al) were heated in the quartz tube at temperature of $850 \text{ }^\circ\text{C}$. BDD substrates were placed downstream from the source to the other end of the tube at around $500 \text{ }^\circ\text{C}$. The experiments were under a constant pressure of $6 \times 10^4 \text{ Pa}$. After evaporation and growth, the samples were drawn out and cooled to room temperature (RT). To obtain the *n*-ZnO NRs/*p*-diamond heterojunction, a transparent conductive indium-tin-oxide (ITO) glass was pressed on the top of ZnO NRs as the electrode and Ag were employed as electrodes for *p*-diamond.

The structures and morphologies of the as-synthesized products were characterized by means of X-ray diffraction (XRD, by RigakuD/MAX-RA with Cu $K\alpha$ radiation of 1.54056 \AA), Raman spectroscopy (by a Renishaw in Via Raman spectrometer with the 514.5 nm line of an Ar^+ ion laser) and scanning electron microscope (SEM, by JEOL JXA-8200 electron probe micro-analyzer). *I*-*V* characteristics of the heterojunction structures were measured by a Keithley 2400 source meter both in dark and under illumination at 365 nm . A UV lamp with a power density of 30 W deuterium lamp was used as the excitation source during photocurrent

measurements. The SPV of samples were measured by surface photovoltage spectrometer (SPS). The instrument was self-assembled. The above examinations are all carried out at room temperature.

3. Results and discussion

Figs. 1a and 1b show the SEM images of the BDD film and ZnO NRs on the BDD film, respectively. The flat BDD film consists of small grains with a diameter of $\sim 1.5 \mu\text{m}$. ZnO NRs are uniformly grown mostly aligned vertically with the diamond substrate. The diameter of the hexagonal nanorods is approximately 500 nm with a length of about 2 μm . Figs. 1c and 1d show the XRD and Raman spectral results of the ZnO NRs grown on BDD film. In the XRD spectrum (Fig. 1c), the main diffraction peaks can be indexed as hexagonal wurtzite structure of ZnO with the lattice parameters $a=3.241 \text{ \AA}$ and $c=5.185 \text{ \AA}$, the peaks presented at 44.1° and 75.5° are assigned to (111) and (220) diffraction peaks of diamond substrates. In Raman spectrum (Fig. 1d), besides the peak at 1328 cm^{-1} originating from diamond with respect to the intrinsic zone-centre phonon band,²⁰ a strong peak appears at 437 cm^{-1} corresponding to the E_2 mode of wurtzite phase of ZnO.²¹ The results of XRD and Raman spectroscopy confirm that the ZnO nanorods grown on BDD are with high quality and mainly along the [0001] direction.

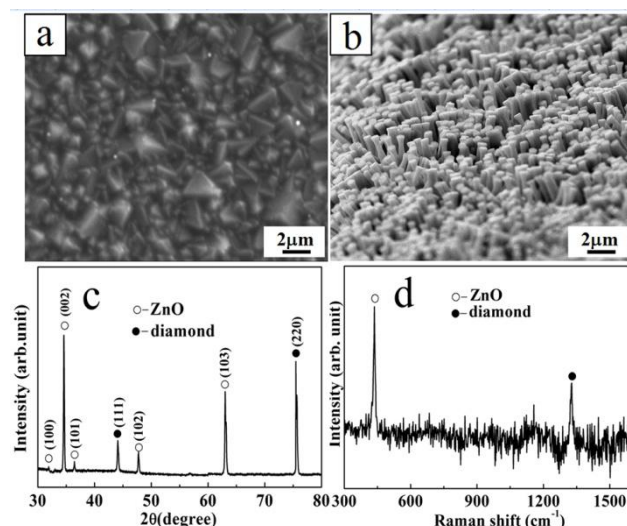


FIG. 1. (a) SEM image of the BDD film and (b) ZnO nanorods grown on the BDD film. (c) and (d)

XRD and Raman spectrum of ZnO nanorods grown on the BDD film.

Fig. 2a schematically depicts the fabricated ZnO NRs/diamond heterojunction device. The linear I - V characteristics of Ag contacts on BDD (Fig. 2b) suggest the ohmic contact. Since the work function of ITO electrode is 4.5 eV and the electron affinity of ZnO is also 4.5 eV, the ZnO-ITO contact is ohmic.²² The unintentionally doped ZnO shows n -type, while the BDD film is p -type. Examined by Hall-effect measurements, the carrier density and the mobility of the p -type BDD in this work are $1.2 \times 10^{19}/\text{cm}^3$ and $12.7 \text{ cm}^2/\text{Vs}$, respectively.

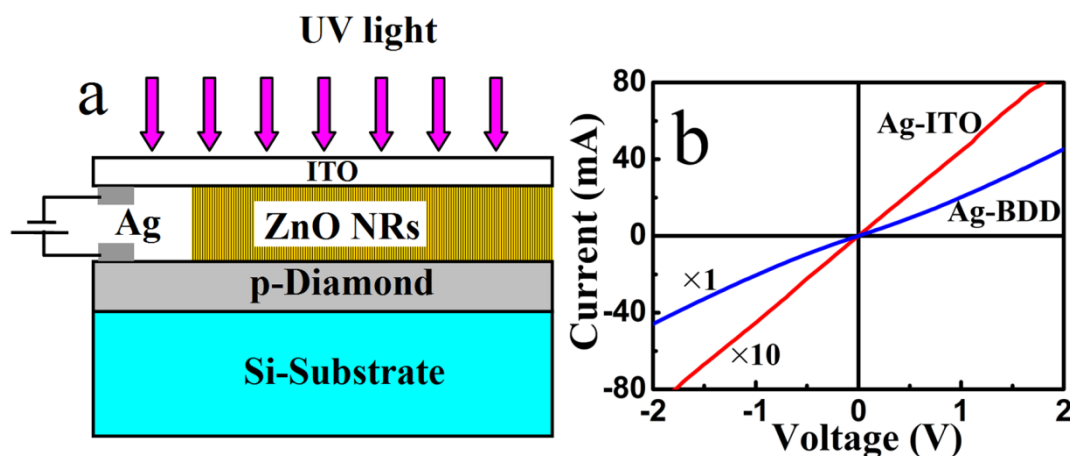
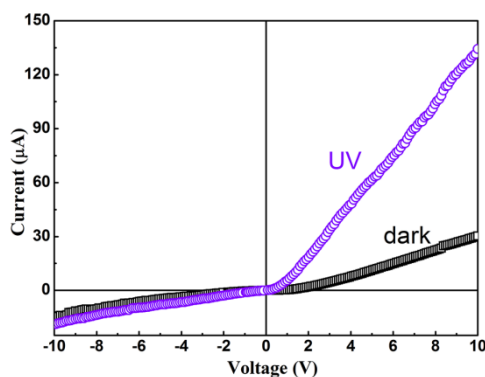


FIG. 2. (a) Schematic diagram of the n -ZnO NRs/ p -diamond heterojunction; (b) Ohmic contacts of Ag/BDD and Ag/ZnO.

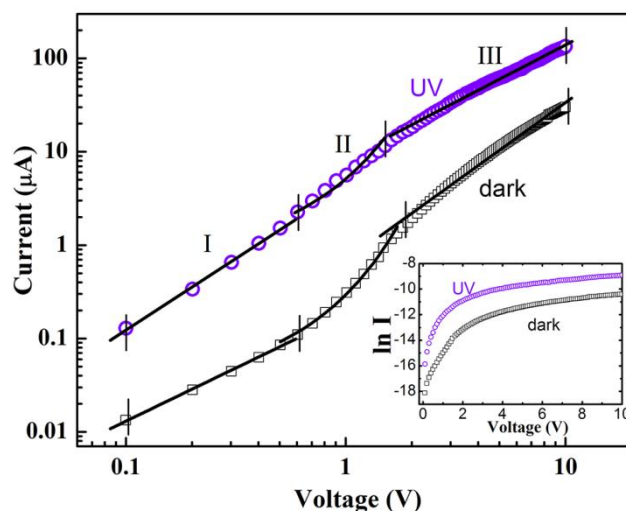
Fig. 3 shows the current-voltage (I - V) characteristics of the synthesized ZnO nanorods on BDD both in the dark and upon UV light illumination with a wavelength of 365 nm using a deuterium lamp. It shows typical rectifying behavior with a rectification ratio of 3.2 and 8.8 for the dark current and the photocurrent, respectively. For the dark, the turn on voltage is 2.15 V and the reverse leakage current is 4 μ A at -5 V, respectively. The large leakage current was mainly due to tunneling effect caused by the high defect concentration or trap centers in the interfacial layer.²³ Under UV illumination, the turn on voltage is lowered to a value of 0.8 V, indicating that the generation of more electrons under UV illumination leads the turn on voltage of the device to lower values.²³ It is noted that the forward current increases significantly with the forward bias. When the forward bias increases to 10 V, the forward current increases from 30 μ A in the dark to 135 μ A under UV illumination, which is more than 4 times higher than the dark current. The turn on voltage of both the dark and the UV illumination are lower than the value of 4 V on the ZnO film/diamond structure.¹⁸ In addition, the dark and photocurrent are about 10^3 times larger than the reported ZnO film/diamond heterojunction.^{17, 18} As a result of the larger surface area to volume ratio¹⁹ and the presence of deep level surface trap states²⁴ in one-dimensional ZnO NRs, the transport and photoconduction properties of the heterojunction are drastically affected and thus can enhance the performance of ZnO NRs/diamond UV photodiodes. On the contrary, the reverse current shows a slower increase. The leakage current is 14.6 μ A at a reverse bias of -10 V, and it increases to 19.6 μ A under light illumination. The results indicate that the ZnO nanorods/diamond heterojunction device is sensitive to the UV light and can be used as a good UV photoelectrical detector.



View Article Online
DOI: 10.1039/C5RA06054K

FIG. 3. I - V characteristics of n -ZnO NRs/ p -diamond heterojunction under the dark and UV illumination, respectively.

Fig. 4 shows the log-log scale plot of the I - V data of the device measured in the dark and under the UV illumination. Both curves can be divided into three distinct regions depending on the applied voltage. At a very low bias voltage for $V < 0.5$ V (region I), a linear dependence of the current on the voltage is observed, suggesting a transport mechanism obeying the Ohmic law.²⁵ At a moderately higher junction voltage (region II, 0.5 V $< V < 1.6$ V), the current exponentially increases and it follows the equation $I \sim \exp(\alpha V)$, which is usually observed in the wide band gap p - n diodes due to the recombination-tunneling mechanism.²⁶⁻²⁸ By fitting the experimental data, the constant α has been evaluated to be 2.33 V⁻¹ and 2.01 V⁻¹ for the dark and under the UV illumination, respectively. Both injection efficiency values are close to the one of ideal vacuum diode of 1.5 V.²⁹ The enlargement of α for the ZnO NRs/diamond p - n junction can be attributed to the more thermally excited carriers.³⁰ When $V > 1.6$ V (region III), the I - V characteristic follows a power law $I \sim V^2$ which is generally attributed to a space-charge-limited current (SCLC) conduction for single-carrier (holes) injection behavior observed in wide band gap semiconductors.³¹⁻³³



View Article Online
DOI: 10.1039/C5RA06054K

FIG. 4. Log-log plots of the I - V characteristics of n -ZnO NRs/ p -diamond heterojunction under the dark and UV illumination. (Inset: the plots of the $\ln(\text{current})$ vs voltage).

A semilog plot of current density versus bias voltage is shown in the inset of Fig. 4.

According to the current-voltage characteristics of the real diodes equation,

$$I = I_s \left[\exp\left(\frac{qV}{nkT}\right) - 1 \right]$$

where I_s is the reverse saturation current, V is the applied voltage, k is the Boltzmann constant, T is the absolute temperature. The ideality factor n of the heterojunction in the dark and under UV illumination is estimated to be 13.8 and 9.8, respectively. The value of ideality factor is larger than 2, indicating that the diode is not an ideal one. Although the ideality factor in the present work is slightly higher than the value obtained in the sputtered CuO/ZnO³⁴ and Si/ZnO²⁵ heterojunctions at low voltage, it is much better than the one obtained in the Si/ZnO junction²⁵ when the voltage is above 1.5 V. This can be attributed to the lattice mismatch between ZnO and diamond due to the presence of surface states.²⁵ The high value of ideality factor is attributed to the space-charge limited conduction, deep-level-assisted tunneling, or parasitic rectifying junctions within the device,³⁵ indicating that the conduction is dominated

by non-thermionic process. The n value under UV illumination is smaller than the dark one and can be explained as follows: under the UV light, more carriers were excited, the tunneling effect through the barrier and the generation-recombination process occurring in the depletion region of ZnO NRs/diamond heterojunction were then enhanced.³⁶

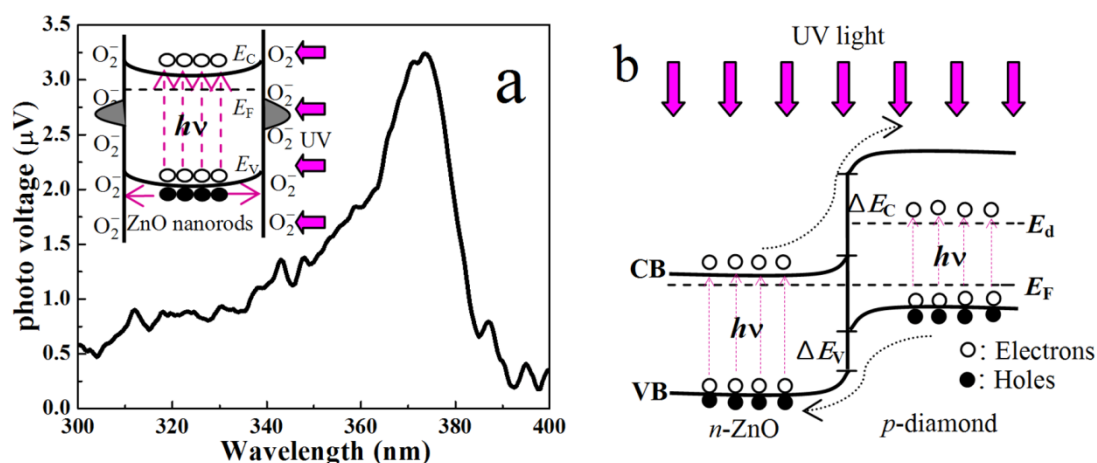


FIG. 5. (a) SPV measurement of the n -ZnO NRs/ p -diamond heterojunction devices. Inset: scheme of the process of electron-holes separation of ZnO NRs with the absorption of O_2 . (b) the energy band diagram of the heterojunction under UV light. ΔE_C is the conduction band offset, ΔE_V is the valence band offset; E_F , the Fermi energy; CB, conduction band; VB, valence band. E_d , donor level of diamond.

To explore the photovoltaic properties of the ZnO NRs / p -diamond heterojunction devices, the SPV measurements were carried out. As shown in Fig. 5, there is a broad photovoltaic response band in the range of 300-400 nm which is in consistent with the UV absorption region of the sample. It can be concluded that this band comes from two different mechanisms, the band to band transition (300-360 nm) and the excitation transition (370-390 nm), respectively.³⁷ The UV SPV photoresponse can be attributed to the oxygen related trap states at the surface of ZnO NRs.^{24, 37} In the air, the n -type conduction of ZnO can make part of the absorbed O_2 negatively charged, then producing a built-in potential at the surface of the as-grown ZnO NRs. When the UV light is absorbed by the ZnO NRs, the electron-hole pairs

are then generated. Most of the photogenerated electron-hole pairs separated and diffuse under the effect of the built in electric field caused by the absorbed oxygen captured holes.³⁷ The built-in potential prevents the carrier recombination and prolongs the lifetime of photo-excited carriers, leading to more electrons excited to the conduction band and injected to the diamond side. Thus, the photo-current of the ZnO/diamond heterojunction can be effectively enhanced when illuminated by the UV energy.

Besides, there exists another important mechanism that affects the photoresponse of the ZnO/diamond heterojunction, which can be explained using the energy band diagram according to Anderson' model, as shown in Fig 5b. The injection current is dominated mainly by the holes in the valence band as the conduction band offset ΔE_C is over two times larger than the valence band offset ΔE_V . The relevant mechanism has been reported in our previous works.^{30,38} When the heterojunction is irradiated by the UV light, on the ZnO side, the electrons in the valence band are excited to the conduction band by absorbing the photon with the wavelength of 365 nm that is corresponding to the bandgap of ZnO, leading to the concentration increase of the electrons carriers. The build-in electric field drives the photogenerated electrons excited to the conduction band of the diamond. While on the diamond side, the electrons will be excited to the shallow donor level of diamond which has lower energy gap of about 2.56 eV studied by thermoluminescence,³⁹ other than to the conduction band of diamond with larger bandgap of 5.5 eV, leaving more holes in the valence band of diamond compared to dark. The photogenerated holes shifted to the ZnO valence band, and the photocurrent was thus enhanced.

View Article Online
DOI: 10.1039/C5RA06054K

RSC Advances Accepted Manuscript

4. Conclusion

In summary, the UV photoresponse properties of n-ZnO nanorods/p-diamond heterojunction have been investigated. The turn on voltage and the ideality factor of the device under UV illumination is lowered. The forward current under UV illumination is more than 4 times higher than the dark one at 10 V. Due to the highest thermal conductivity, wide band gap, high radiation resistance, good chemical and temperature stability, diamond is presumed to be an ideal heat exchange material (such as heat sink and heat spreader), which can be used at high temperature, high flux and other severe environments. It is proposed that the valid combination of the two wide-band gap semiconductors would be a way to realize the UV photoconductor devices.

Acknowledgements

This work was financially supported by the National Natural Science Foundation of China (Grant Nos. 51472105, 51072066, 11347154 and 1172194), the Ph.D. Programs Foundation of Ministry of Education of China (Grant No. 20100061110083) and the Foundation of Xuzhou Institute of Technology, China (Grant No. XKY2013203).

- 1 L. Ji, S. Peng, Y.-K. Su, S.-J. Young, C. Wu and W. Cheng, *Appl. Phys. Lett.*, 2009, **94**, 203106. DOI: 10.1039/C5RA06054K
- 2 Y. Tu, L. Zhou, Y. Z. Jin, C. Gao, Z. Z. Ye, Y. F. Yang and Q. L. Wang, *J. Mater. Chem.*, 2010, **20**, 1594.
- 3 J. B. Baxter and E. S. Aydil, *Appl. Phys. Lett.*, 2005, **86**, 053114.
- 4 X. M. Zhang, M. Y. Lu, Y. Zhang, L. J. Chen and Z. L. Wang, *Adv. Mater.*, 2009, **21**, 2767.
- 5 Y. I. Alivov, U. Ozgur, S. Dogan, D. Johnstone, V. Avrutin, N. Onojima, C. Liu, J. Xie, Q. Fan and H. Morkoc, *Appl. Phys. Lett.*, 2005, **86**, 241108.
- 6 L. Duan, P. Wang, F. Wei, X. Yu, J. Fan, H. Xia, P. Zhu and Y. Tian, *J. Alloy. Compd.*, 2014, **602**, 290.
- 7 S. Mridha, M. Dutta and D. Basak, *J. Mater. Sci: Mater. El.*, 2009, **20**, 376.
- 8 L. Su, Q. Zhang, T. Wu, M. Chen, Y. Su, Y. Zhu, R. Xiang, X. Gui and Z. Tang, *Appl. Phys. Lett.*, 2014, **105**, 072106.
- 9 M. Ding, D. Zhao, B. Yao, Z. Li and X. Xu, *RSC Adv.*, 2015, **5**, 908.
- 10 Y. I. Alivov, U. Ozgur, S. Dogan, D. Johnstone, V. Avrutin, N. Onojima, C. Liu, J. Xie, Q. Fan and H. Morkoc, *Appl. Phys. Lett.*, 2005, **86**.
- 11 H. Ohta, M. Hirano, K. Nakahara, H. Maruta, T. Tanabe, M. Kamiya, T. Kamiya and H. Hosono, *Appl. Phys. Lett.*, 2003, **83**, 1029.
- 12 Y. Shen, X. Yan, Z. Bai, X. Zheng, Y. Sun, Y. Liu, P. Lin, X. Chen and Y. Zhang, *RSC Adv.*, 2015, **5**, 5976.
- 13 P. Lin, X. Chen, X. Yan, Z. Zhang, H. Yuan, P. Li, Y. Zhao and Y. Zhang, *Nano Research*, 2014, **7**, 860.
- 14 O. Game, U. Singh, T. Kumari, A. Banpurkar and S. Ogale, *Nanoscale*, 2014, **6**, 503.
- 15 C. Wang, S. K. Jha, Z. Chen, T. W. Ng, Y. Liu, M. F. Yuen, Z. Lu, S. Y. Kwok, J. A. Zapien and I. Bello, *J. Nanosci. Nanotechnol.*, 2012, **12**, 4560.
- 16 Q. Yu, J. Li, H. Li, Q. Wang, S. Cheng and L. Li, *Chem. Phys. Lett.*, 2012, **539**, 74.
- 17 J. Huang, L. Wang, R. Xu, W. Shi and Y. Xia, *Semicond. Sci. Technol.*, 2008, **23**, 125018.
- 18 K. Saw, S. Tneh, F. Yam, S. Ng and Z. Hassan, *Physica B*, 2010, **405**, 4123.
- 19 G. Chai, O. Lupan, L. Chow and H. Heinrich, *Sens. Actuators, A*, 2009, **150**, 184.
- 20 A. Ferrari and J. Robertson, *Phys. Rev. B*, 2000, **61**, 14095.
- 21 M. Rajalakshmi, A. K. Arora, B. Bendre and S. Mahamuni, *J. Appl. Phys.*, 2000, **87**, 2445.
- 22 Y. Yang, Q. Liao, J. Qi, Y. Zhang, L. Tang and N. Ye, *Appl. Phys. Lett.*, 2008, **93**, 133101.
- 23 S.-Y. Liu, T. Chen, Y.-L. Jiang, G.-P. Ru and X.-P. Qu, *J. Appl. Phys.*, 2009, **105**, 114504.
- 24 C. Soci, A. Zhang, B. Xiang, S. A. Dayeh, D. Aplin, J. Park, X. Bao, Y.-H. Lo and D. Wang, *Nano Lett.*, 2007, **7**, 1003.
- 25 N. Koteeswara Reddy, Q. Ahsanulhaq, J. H. Kim and Y. Hahn, *Appl. Phys. Lett.*, 2008, **92**, 043127.
- 26 J. Ye, S. Gu, S. Zhu, S. Liu, R. Zhang, Y. Shi and Y. Zheng, *Appl. Phys. Lett.*, 2006, **88**, 182112.
- 27 M. Dutta and D. Basak, *Appl. Phys. Lett.*, 2008, **92**, 212112.
- 28 J. Fedison, T. Chow, H. Lu and I. Bhat, *Appl. Phys. Lett.*, 1998, **72**, 2841.
- 29 R. Forman, *Physical Review*, 1961, **123**, 1537.
- 30 D. Sang, H. Li, S. Cheng, Q. Wang, Q. Yu and Y. Yang, *J. Appl. Phys.*, 2012, **112**, 036101.
- 31 M. Jayaraj, A. Draeseke, J. Tate, R. Hoffman and J. Wager, in *Transparent pn Heterojunction Thin Film Diodes*, 2001 (Cambridge Univ Press), p. F4. 1.
- 32 Y. I. Alivov, J. Van Nostrand, D. C. Look, M. Chukichev and B. Ataev, *Appl. Phys. Lett.*, 2003, **83**, 2943.
- 33 I.-S. Jeong, J. H. Kim and S. Im, *Appl. Phys. Lett.*, 2003, **83**, 2946.
- 34 S. Mridha and D. Basak, *Semicond. Sci. Technol.*, 2006, **21**, 928.
- 35 D. Norton, M. Ivill, Y. Li, Y. Kwon, J. Erie, H. Kim, K. Ip, S. Pearton, Y. Heo and S. Kim, *Thin Solid Films*, 2006, **496**, 160.
- 36 S. Majumdar and P. Banerji, *J. Appl. Phys.*, 2009, **105**, 043704.

37 Y. Lin, D. Wang, Q. Zhao, Z. Li, Y. Ma and M. Yang, *Nanotechnology*, 2006, **17**, 2110.

View Article Online
DOI: 10.1039/C5RA06054K

38 H. Li, D. Sang, S. Cheng, J. Lu, X. Zhai, L. Chen and X.-Q. Pei, *Appl. Surf. Sci.*, 2013, **280**, 201.

39 M. Benabdesselam, P. Iacconi, F. Wrobel, A. Petitfils and J. Butler, *Diam. Relat. Mater.*, 2007, **16**, 805.

RSC Advances Accepted Manuscript